

MINISTRY OF EDUCATION
AND TRAINING

VIETNAM ACADEMY OF
SCIENCE AND TECHNOLOGY

GRADUATE UNIVERSITY OF SCIENCE AND TECHNOLOGY



NGO KHAC KHONG MINH

**SYNTHESIS AND STUDYING ON
OPTICAL PROPERTIES OF Ln_3PO_7 ($\text{Ln}=\text{La}, \text{Gd}$)
NANOMATERIALS DOPED WITH Eu^{3+} IONS**

**SUMMARY OF DISSERTATION ON
OPTICAL MATERIALS, OPTOELECTRONICS AND
PHOTONICS**

Code: 9 44 01 27

Hanoi, 2024

The dissertation is completed at: Graduate University of Science and Technology, Vietnam Academy Science and Technology

Supervisors:

1. Supervisor 1: Dr. Nguyen Vu
2. Supervisor 2: Dr. Lam Thi Kieu Giang

Referee 1: Assoc. Prof. Dr. Le Tien Ha

Referee 2: Assoc. Prof. Dr. Nguyen Van Quy

Referee 3: Assoc. Prof. Dr. Nguyen Tu

The dissertation is examined by Examination Board of Graduate University of Science and Technology, Vietnam Academy of Science and Technology at..... (time, date.....)

The dissertation can be found at:

1. Graduate University of Science and Technology Library
2. National Library of Vietnam

INTRODUCTION

Until now, phosphate-based luminescent nanomaterials doped with rare earth ions have attracted attention from many research groups because of interesting properties such as: long-lasting emission effect, fluorescence quenching level according to temperature. low, quantum efficiency is high. As is known, the La^{3+} ion has a $4f^0$ configuration, so it does not affect the fluorescence of the central ion. Besides, Gd^{3+} ions have a semi-saturated electron shell configuration of $4f^7$, and have strong paramagnetic properties - meaning they become magnetic when placed in an external magnetic field. Furthermore, the level transition energy with charge transfer and f - f transition energy of Gd^{3+} ion is higher than that of other rare earth elements, so it does not cause fluorescence quenching for other rare earth ions. Therefore, phosphate-based luminescent materials of La^{3+} and Gd^{3+} have many extremely interesting properties. In the $\text{Ln}_2\text{O}_3\text{-P}_2\text{O}_5$ network system, the materials that have been focused on research are LnPO_4 , Ln_3PO_7 , LnP_3O_9 ... Currently, the material $\text{LnPO}_4\text{:Eu}$ has received the attention of scientists in Vietnam in particular. and the world in general. However, up to now, the number of research projects on $\text{Ln}_3\text{PO}_7\text{:Eu}$ material in the world is very small and there have been no research projects on this material in Vietnam. Therefore, $\text{Ln}_3\text{PO}_7\text{:Eu}$ is the object we chose to research to find the optimal conditions for synthesizing the material.

There are many methods to prepare nanoparticle materials such as solid phase reaction method, sol-gel method, co-precipitation method, explosive reaction method... In 2008, Ye Jin and his colleagues synthesized Successfully combined La_3PO_7 material by explosive reaction, using glycine as an agent for redox reaction. Recently, author Nguyen Vu's research group has also successfully manufactured gadolinium phosphate and gadolinium oxide materials by explosive reaction method, using urea as the agent. Therefore,

we chose the explosive reaction method to prepare the material, using urea as the agent for the redox reaction because this is one of the simple methods to obtain materials with high reaction size. nanometer size, making it possible to synthesize materials on a large scale.

The birth of the Judd-Ofelt theory marked a turning point in the study of optical properties of rare earth ions. The important content of the Judd-Ofelt theory is the calculation of intensity parameters ($\Omega = 2, 4, 6$), these parameters only depend on the background lattice and rare earth ions and do not depend on any specific transition and is calculated from the absorption and fluorescence spectra. With only these three parameters, we can evaluate the asymmetry of the crystal field as well as the binding properties between rare earth ions and the background lattice. In addition, from intensity parameters, we can also use it to predict other optical properties of materials such as transition probability, lifetime, quantum efficiency, fluorescence branching ratio. Based on these optical parameters, we can know the applicability of the material.

From the analysis and evaluation of the research results of scientists on luminescent materials with a main lattice of Ln_3PO_7 ($\text{Ln}=\text{La, Gd}$), we chose the topic "*Synthesis and studying the optical properties of nanomaterial Ln_3PO_7 ($\text{Ln}=\text{La, Gd}$) doped with Eu^{3+} ions*" to continue researching factors that have not been mentioned in previous published works.

Research purpose:

- Announcing the synthesis process of luminescent nanomaterial $\text{Ln}_3\text{PO}_7:\text{Eu}^{3+}$ ($\text{Ln} = \text{La, Gd}$) on a laboratory scale and factors to improve the luminescent properties of the material (reaction temperature, ion concentration doped with Eu^{3+} and Bi^{3+} sensitizing ion).

- Compare the optical properties between materials in the $\text{Ln}_2\text{O}_3\text{-P}_2\text{O}_5$ ($\text{Ln}=\text{La}, \text{Gd}$) lattice system doped with Eu^{3+} ions using intensity and emission parameters to guide the application of red light irradiation.

Main tasks of the thesis:

- Research on manufacturing luminescent nanomaterials doped with Eu^{3+} by explosive reaction method, using urea as fuel.

- After being synthesized, the structure, morphology and optical properties of the materials are studied.

- Investigate the influence of factors: temperature, doping concentration on the formation and properties of materials. From there, find the optimal conditions to synthesize materials.

- Research on the influence of Bi^{3+} sensitizing ion on the optical properties of $\text{Ln}_3\text{PO}_7:\text{Eu}^{3+}$ material.

- Applying Judd-Ofelt theory to calculate optical parameters of materials.

The thesis provides an overall view of the synthesis and enhancement of luminescent properties to create nanometer-sized luminescent substances based on La_3PO_7 , Gd_3PO_7 activated by rare earth ions Eu^{3+} , investigating the effects of sensitizing ions Bi^{3+} .

New points of the thesis:

-Synthesized luminescent nanomaterials $\text{La}_3\text{PO}_7:\text{Eu}^{3+}$, $\text{Gd}_3\text{PO}_7:\text{Eu}^{3+}$ by explosive reaction method, using urea as fuel.

-Research on the effects of factors: synthesis temperature, doping ion concentration on the optical properties of two materials $\text{La}_3\text{PO}_7:\text{Eu}^{3+}$, $\text{Gd}_3\text{PO}_7:\text{Eu}^{3+}$.

-Study the influence of Bi^{3+} ions on the optical properties of two materials $\text{La}_3\text{PO}_7:\text{Eu}^{3+}$, $\text{Gd}_3\text{PO}_7:\text{Eu}^{3+}$.

-Compare the optical properties between materials in the $\text{Ln}_2\text{O}_3\text{-P}_2\text{O}_5$ ($\text{Ln}=\text{La}, \text{Gd}$) doped Eu^{3+} lattice system with specific data by applying the Judd-Ofelt theory

Layout of the thesis:

In addition to the introduction, conclusion, list of symbols and abbreviations, list of tables, list of images and drawings, list of published works related to the thesis and references, the thesis content is presented in 4 chapters:

Chapter 1: Overview of nanomaterials containing luminescent rare earth ions based on Ln_3PO_7

Chapter 2: Experiment and research methods

Chapter 3: Research on the structure and optical properties of $\text{Gd}_3\text{PO}_7\text{:Eu}^{3+}$ nanomaterials

Chapter 4: Research on the structure and optical properties of $\text{La}_3\text{PO}_7\text{:Eu}^{3+}$ nanomaterial

The main results of the thesis have been published in 2 international scientific works on the ISI list and 2 prestigious domestic scientific works.

CHAPTER 1. OVERVIEW

1.1 Nanomaterials

1.2 Fluorescent materials

1.3 Luminescent nanomaterials containing rare earth ions

1.3.1 Electronic shell structure and optical properties of trivalent rare earth ions

1.3.2 Overview of 4f energy level

1.3.3 Optical absorption transitions in the energy range of the 4f levels

1.3.4 Fluorescence quenching due to doping ion concentration

1.4 Judd-Ofelt theory

1.5 Overview of Ln_3PO_7 material

1.5.1 Influence of the host lattice on the fluorescence properties of Eu^{3+} ions

1.5.2 Research projects on Ln_3PO_7 material 1.1 Vật liệu nano

CHAPTER 2: EXPERIMENTAL

2.1 Method of manufacturing material $\text{Ln}_3\text{PO}_7:\text{Eu}^{3+}$ ($\text{Ln}=\text{La}, \text{Gd}$)

2.1.1 Solid phase reaction method

2.1.2 Sol-gel method

2.1.3 Hydrothermal method

2.1.4 Explosive reaction method

2.2 Manufacturing material $\text{Ln}_3\text{PO}_7:\text{Eu}^{3+}$ ($\text{Ln}=\text{La}, \text{Gd}$) by explosive reaction method

Material $\text{Ln}_3\text{PO}_7: 5\% \text{Eu}^{3+}$ ($\text{Ln}=\text{La}, \text{Gd}$) is made by explosive reaction method (according to the process described in figure 2.1) from precursors $\text{Ln}(\text{NO}_3)_3$, $\text{Eu}(\text{NO}_3)_3$, H_3PO_4 , NH_3 and use urea as fuel for oxidation-reduction reactions.

First, take a suitable amount of metal nitrate salt solution in the material into a glass cup and evaporate to remove all residual acid (the evaporation process is repeated 3 times). After the third evaporation, the mixture of nitrate salts of metals was dissolved into a solution with 2 ml of water. To this salt solution, add 0.3 grams of urea, boil for 30 minutes at 70°C , with magnetic stirring and a lid, to obtain colorless solution 1.

In another cup, dissolve 2M NH_3 solution and 0.5M H_3PO_4 solution in a molar ratio of 1:1. The above mixture was stirred for 30 minutes to obtain colorless solution 2.

Then solution 2 above was slowly dripped into solution 1 and a white cloud appeared. This mixture is further boiled for 30 minutes, at 70°C , with a lid. Then, remove the lid, take out the magnetic stirrer and continue to evaporate to obtain a precursor sample of the material. The precursor sample of the

material is dried at 80°C, then preheated at 500°C for 30 minutes with a heating rate of 10°C/min.

After preheating at 500°C, the material is crushed, then divided into 5 parts and heated at different temperatures from 500 - 900°C for 1 hour with a heating rate of 10°C/min to obtain the material.

2.3 Methods for determining the structure, micromorphology and optical properties of materials

2.3.1 Thermal analysis method

2.3.2 Infrared spectroscopy method

2.3.3 X-ray diffraction method

2.3.4 Micromorphological study by scanning electron microscope (SEM)

2.3.5 Transmission electron microscopy (TEM)

2.3.6 Fluorescence spectroscopy method

2.3.7 Method for determining fluorescence lifetime

CHAPTER 3: STUDYING THE STRUCTURE AND OPTICAL PROPERTIES OF $Gd_3PO_7:Eu^{3+}$ NANO MATERIALS

3.1. Structure and morphology of $Gd_3PO_7:Eu^{3+}$ material

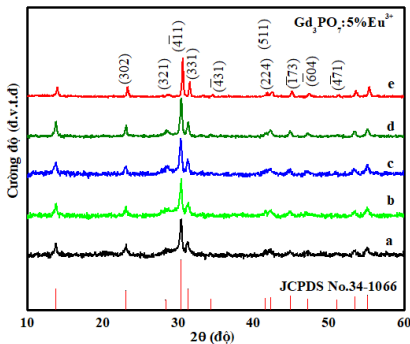


Figure 3.2. X-ray diffraction pattern of $Gd_3PO_7:5\%Eu^{3+}$ synthesized at different temperatures: 500°C(a), 600°C(b), 700°C(d), 800°C(d), 900°C(e)

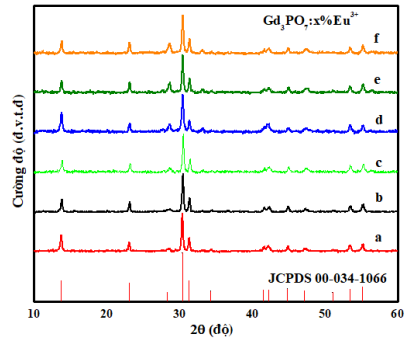


Figure 3.1. X-ray diffraction pattern of Gd_3PO_7 samples: $x\%Eu^{3+}$ at 900°C ($x=0.1$ (a), 1(b), 3(c), 5(d), 7(e), 9(f))

X-ray diffraction patterns of $\text{Gd}_3\text{PO}_7: 5\% \text{Eu}^{3+}$ material samples with synthesis temperatures from 500 to 900°C are presented in Figure 3.2. The results show that the crystalline phase of the Gd_3PO_7 matrix has been recorded: the sample received is single phase, the crystal structure is good, the diffraction lines are consistent with the JCPDS 34 - 1066 standard card, the appearance of of doping. All diffraction peaks characterize the structure of the monoclinic crystalline phase. X-ray diffraction pattern of $\text{Gd}_3\text{PO}_7:x\% \text{Eu}^{3+}$ sample with different doping ion concentrations ($x = 0.1, 1, 3, 5, 7, 9$) is presented in Figure 3.3. The average crystal sizes of $\text{Gd}_3\text{PO}_7:x\% \text{Eu}^{3+}$ material samples with $x = 0.1, 1, 3, 5, 7, 9$ are 24, 24, 25, 24, 25 and 26 nm, respectively. It is clear that the average crystallite size of the material samples has almost no significant change.

SEM images of two $\text{Gd}_3\text{PO}_7:5\% \text{Eu}^{3+}$ material samples (Figure 3.6) show that the material particles have a spherical shape when heated at 500 and 900°C, with fairly uniform sizes, the size of the material particles is about 20-30 nm.

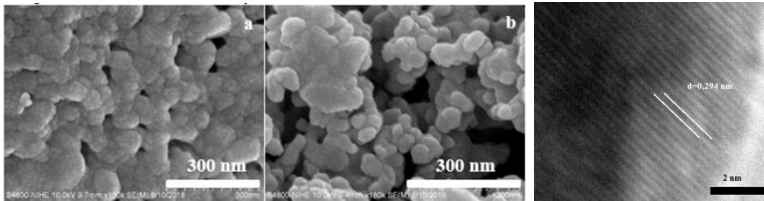


Figure 3. 3 SEM images of $\text{Gd}_3\text{PO}_7:5\% \text{Eu}^{3+}$ material heated at 500°C (a) and 900°C (b)

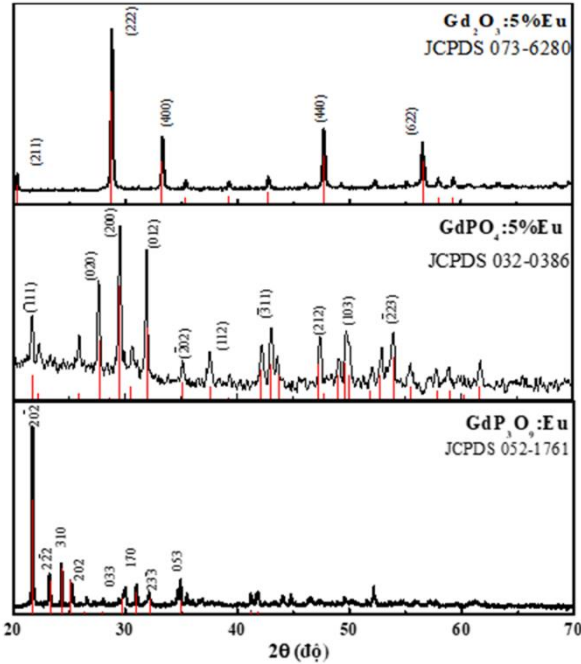


Figure 3. 4 X-ray diffraction patterns of material samples $\text{Gd}_2\text{O}_3:5\%\text{Eu}$, $\text{GdPO}_4:5\%\text{Eu}$ and $\text{GdP}_3\text{O}_9:5\%\text{Eu}$

X-ray diffraction patterns of three types of materials $\text{Gd}_2\text{O}_3:5\%\text{Eu}$, $\text{GdPO}_4:5\%\text{Eu}$ and $\text{GdP}_3\text{O}_9:5\%\text{Eu}$ are presented in Figure 3.8. The results show that all the synthesized materials are single-phase, with no doping appearing on the diagram. Prove that all materials have been successfully synthesized by explosive reactions.

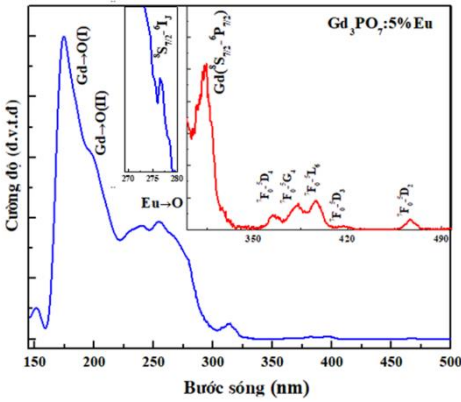
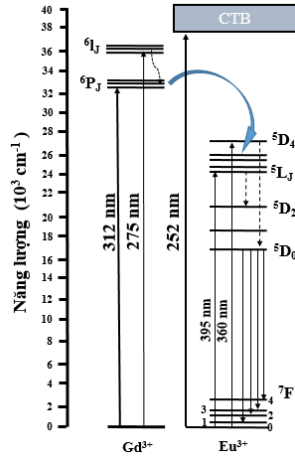


Figure 3. 5 Fluorescence excitation spectrum of $Gd_3PO_7:5\%Eu^{3+}$ material



The fluorescence excitation spectrum of the $Gd_3PO_7:5\%Eu^{3+}$ material is presented in Figure 3.9 corresponding to the emission at wavelength 615 nm including three broad excitation bands and a few narrow lines. The broad band observed around 260 nm is the charge transfer region between O^{2-} and Eu^{3+} . The broad band around 155 nm is believed to be the absorption region of PO_4^{3-} . The absorption signal around 200 nm is the charge transfer region between $Gd \rightarrow O$. The narrow lines in the range from 320 - 550 nm correspond to the f-f transitions of Eu^{3+} .

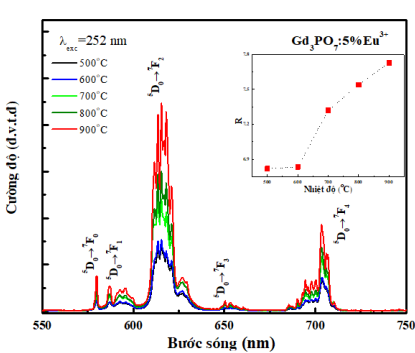


Figure 3.6 Fluorescence spectra of $Gd_3PO_7:5\%Eu^{3+}$ samples synthesized at different

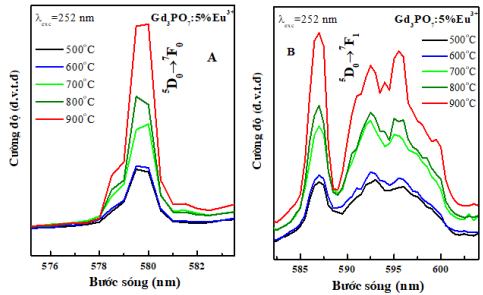


Figure 3. 7 Fluorescence spectra corresponding to the transitions $5D_0 - 7F_0$ (A) and $5D_0 - 7F_1$ (B) of the material $Gd_3PO_7:5\%Eu^{3+}$

The fluorescence spectra of $\text{Gd}_3\text{PO}_7:5\%\text{Eu}^{3+}$ material samples synthesized at different temperatures are presented in Figure 3.11, showing that the $5D_0 \rightarrow 7F_2$ transition has the strongest intensity. Therefore, Eu^{3+} ions occupy non-inverting symmetric center positions in the Gd_3PO_7 matrix. The spectral range from 577 nm to 582 nm corresponding to the $5D_0 - 7F_0$ transition (Figure 3.12A) has two peaks, so there must exist two Eu^{3+} center positions in the Gd_3PO_7 matrix. Besides, observing the fluorescence spectrum of transition $5D_0 - 7F_1$ (Figure 3.12B) shows that there are more than three different luminescence peaks in the emission region of this transition. This result proves that there is more than one Eu^{3+} center site in the Gd_3PO_7 matrix. We calculated the B20 parameter values of $\text{Gd}_3\text{PO}_7:5\%\text{Eu}^{3+}$ samples calcined at 500, 600, 700, 800 and 900°C to be 722, 722, 717, 707 and 704 cm^{-1} , respectively. The B20 value tends to decrease as the sample calcination temperature increases. The B20 parameter of the material $\text{Gd}_3\text{PO}_7:5\%\text{Eu}^{3+}$ has a quite large value. This is the cause of the appearance of the $5D_0 \rightarrow 7F_3$ transition in the emission spectrum of $\text{Gd}_3\text{PO}_7:5\%\text{Eu}^{3+}$

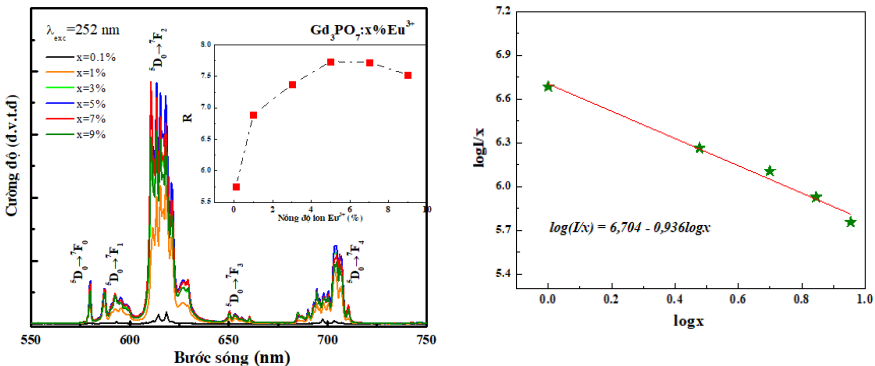


Figure 3.9 Fluorescence spectrum of $\text{Gd}_3\text{PO}_7:x\%\text{Eu}^{3+}$ samples calcined at 900°C

Concentration-induced fluorescence quenching occurs when the Eu^{3+} ion concentration is greater than 5 mol%. The critical distance between Eu^{3+} luminescence centers calculated according to the Blasse formula is 6.039 Å. Figure 3.14 is a graph showing the dependence of $\log(I/x)$ on $\log x$ of the material $\text{Gd}_3\text{PO}_7:x\%\text{Eu}^{3+}$. The results show that the slope coefficient is -0.936, from here we can calculate $Q = 2.808$, this value is close to $Q = 3$. Therefore, it can be said that exchange interaction plays a major role in the extinguishing process. Fluorescent.

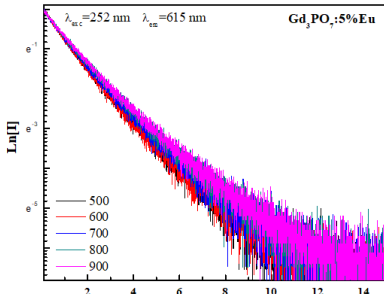


Figure 3.10 Fluorescence attenuation curve of $\text{Gd}_3\text{PO}_7:5\%\text{Eu}^{3+}$ materials calcined at different temperatures

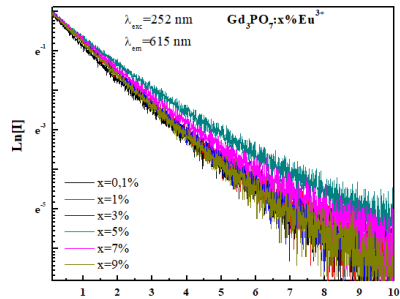


Figure 3.11 Fluorescence attenuation curve of $\text{Gd}_3\text{PO}_7:x\%\text{Eu}^{3+}$ material

It can be seen that the emission time of Eu^{3+} ion in all samples is determined by the equation: $I = A_1\exp(-t/\tau_1) + A_2\exp(-t/\tau_2)$. The fluorescence lifetime of the $\text{Gd}_3\text{PO}_7:5\%\text{Eu}^{3+}$ sample is 1.78 ms.

The branching ratio of the 5D0-7F2 transition for the two materials $\text{Gd}_2\text{O}_3:5\%\text{Eu}^{3+}$ and $\text{Gd}_3\text{PO}_7:5\%\text{Eu}^{3+}$ is very high (both above 70%). Besides, the material $\text{Gd}_3\text{PO}_7:5\%\text{Eu}^{3+}$ has an R value of 7.73, the highest in the $\text{Gd}_2\text{O}_3\text{-P}_2\text{O}_5$ material system. This shows that the $\text{Gd}_3\text{PO}_7:\text{Eu}^{3+}$ material has the highest asymmetry of the ligand field and the highest red emission fluorescence efficiency among the four materials.

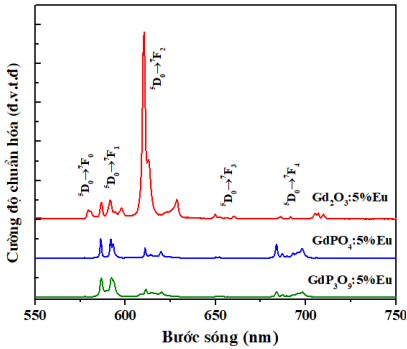


Figure 3. 13 Normalized fluorescence spectra of $\text{Gd}_2\text{O}_3:5\%\text{Eu}^{3+}$, $\text{GdPO}_4:5\%\text{Eu}^{3+}$

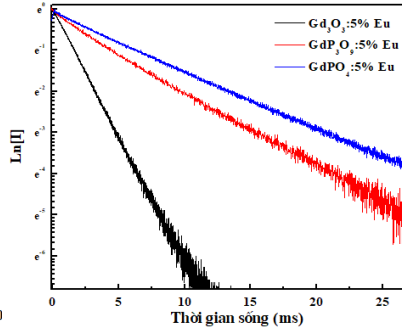


Figure 3. 12 Normalized fluorescence spectra of $\text{Gd}_2\text{O}_3:5\%\text{Eu}^{3+}$, $\text{GdPO}_4:5\%\text{Eu}^{3+}$

The average experimental lifetime result of the $\text{Gd}_2\text{O}_3:5\%\text{Eu}^{3+}$ material is 1.8 ms, which is equivalent to the lifetime of the $\text{Gd}_3\text{PO}_7:5\%\text{Eu}^{3+}$ material (1,785 ms), for the $\text{GdPO}_4:5\%\text{Eu}^{3+}$ sample. quite long with a value of 6.8 ms. The fluorescence lifetime of the $\text{GdP}_3\text{O}_9:5\%\text{Eu}^{3+}$ material is 4.76 ms.

Table 3. 1 Intensity parameters $\Omega\lambda$ of doped Eu^{3+} in $\text{Gd}_2\text{O}_3\text{-P}_2\text{O}_5$ matrix system

Samples	$\Omega_2 (\times 10^{-20} \text{ cm}^2)$	$\Omega_4 (\times 10^{-20} \text{ cm}^2)$
$\text{Gd}_2\text{O}_3:5\%\text{Eu}^{3+}$	6,95	1,16
$\text{Gd}_3\text{PO}_7:5\%\text{Eu}^{3+}$	11,86	5,78
$\text{GdPO}_4:5\%\text{Eu}^{3+}$	1,17	3,70
$\text{GdP}_3\text{O}_9:5\%\text{Eu}^{3+}$	1,02	1,30
$\text{La}_3\text{PO}_7:5\%\text{Eu}$	9,11	3,91
$\text{TiO}_2:5\%\text{Eu}^{3+}$	7,48	4,03
$\text{BaO}.\text{Bi}_2\text{O}_3.\text{B}_2\text{O}_3.\text{Eu}^{3+}$	7,35	3,45
$\text{KLa}(\text{PO}_3)_4:5\%\text{Eu}^{3+}$	1,88	3,54

Calculation results of the strength parameters $\Omega\lambda$ ($\lambda=2.4$) of the $\text{Gd}_2\text{O}_3\text{-P}_2\text{O}_5$ material system show that the Ω_2 value of the materials $\text{GdPO}_4:5\%\text{Eu}^{3+}$, $\text{GdP}_3\text{O}_9:5\%\text{Eu}^{3+}$ has a very low value. However, for the

material Gd₃PO₇:5%Eu³⁺, the Ω_2 value is much larger than the remaining materials in the same matrix system. This proves that the asymmetry of the ligand and the covalency of the Eu³⁺-ligand bond are much larger than those of the compared materials. The calculated Ω_4 value of Gd₃PO₇:5%Eu³⁺ material is 5.78. This result also shows that, among the four materials in the Gd₂O₃-P₂O₅ network system, the Gd₃PO₇:5%Eu³⁺ material has the lowest hardness of the environment around the Eu³⁺ ion.

Observation of the fluorescence excitation spectrum and fluorescence spectrum of samples co-doped with Bi³⁺ ions shows the transfer of resonance energy from Bi³⁺ to Eu³⁺ in the Gd₃PO₇:Eu³⁺ material.

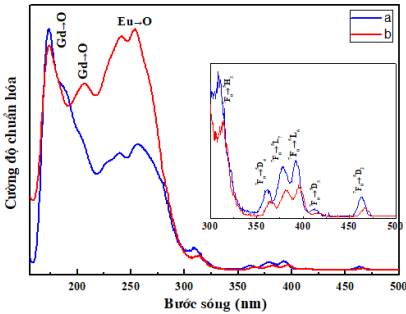


Figure 3.15 Fluorescence excitation spectrum of materials Gd₃PO₇:5%Eu (a) and

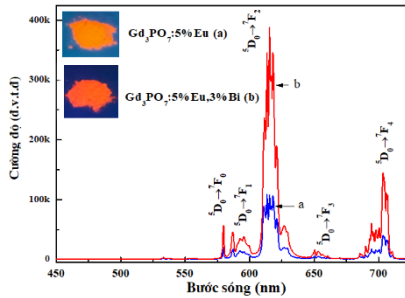


Figure 3.14 Fluorescence spectrum of materials Gd₃PO₇:5%Eu (a) and

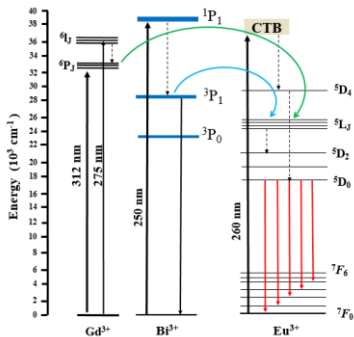


Figure 3.17 Energy transfer diagram of Gd₃PO₇:Eu,Bi

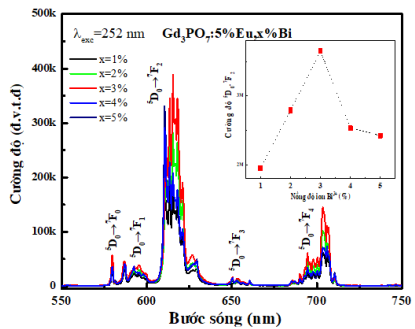


Figure 3.16 Fluorescence spectrum of Gd₃PO₇:5%Eu, x%Bi

In this study, the optimal Bi³⁺ co-doped ion concentration was 3 mol%.

CHAPTER 4: STUDYING THE STRUCTURE AND OPTICAL PROPERTIES OF NANO MATERIAL La₃PO₇:Eu³⁺

The XRD pattern shows that the synthesized material has a good, single-phase crystal structure. Besides, when the temperature increases from 700 to 900°C, the diffraction peaks become narrower and sharper, proving that the crystal is increasingly perfect. All diffraction peaks characterize the structure of the monoclinic crystalline phase.

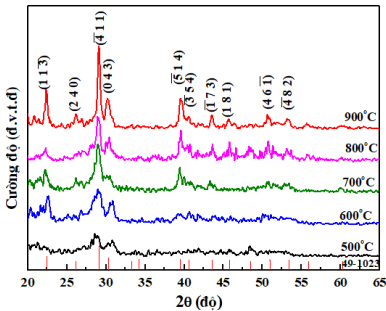


Figure 4. 2 X-ray diffraction pattern of La₃PO₇: 5% Eu³⁺ synthesized at different

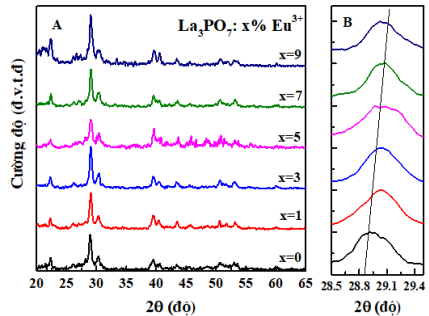


Figure 4. 1 X-ray diffraction pattern of La₃PO₇ samples: x% Eu³⁺ at 800°C

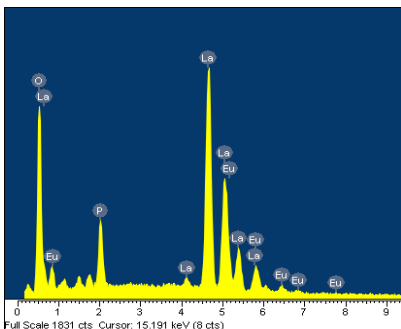


Figure 4. 4 EDX analysis results of La₃PO₇:5%Eu³⁺ material

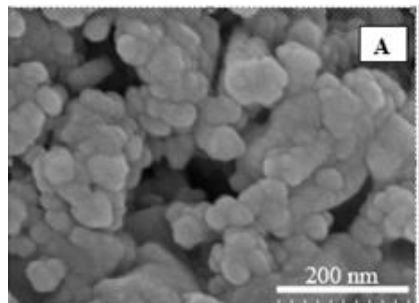


Figure 4. 4 EDX analysis results of La₃PO₇:5%Eu³⁺ material

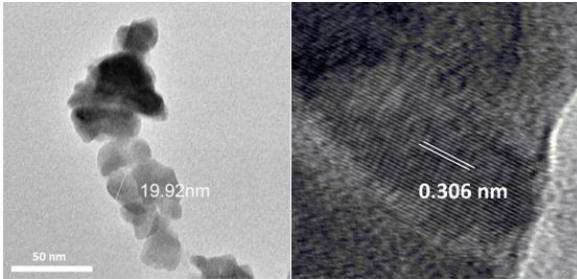


Figure 4. 5 HR-TEM and X-ray diffraction pattern of La₃PO₇:5%Eu³⁺ material

The material particles have a spherical shape and are quite uniform in size. The size of the material particles is about 10-20 nm. HR-TEM measured the distance between neighboring planes to be 0.306 nm corresponding to the ($4\bar{1}1$) plane of monoclinic La₃PO₇ crystal.

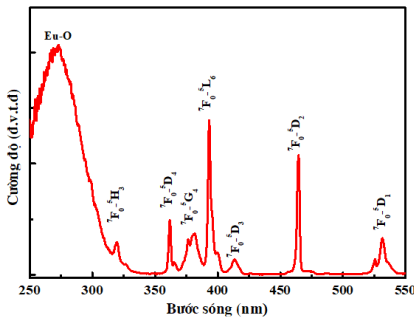


Figure 4. 6 Fluorescence excitation spectrum of La₃PO₇:5%Eu³⁺ material

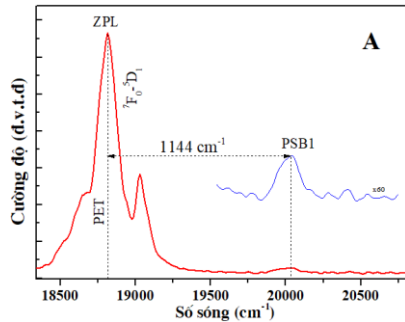


Figure 4. 7 Sideband phonon spectrum of 7F₀→5D₂ transitions

The calculation result of the electron-phonon coupling parameter (g) corresponding to the 7F₀→5D₁ transition is 0.0179. When the g value is smaller, the electron - phonon interaction is poor, meaning the probability of emission transition is large, causing the luminescence intensity to increase.

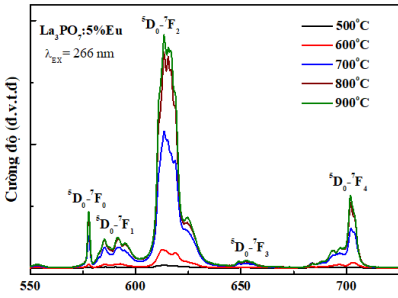


Figure 4. 9 Fluorescence spectra of La3PO7:5%Eu3+ samples synthesized at different

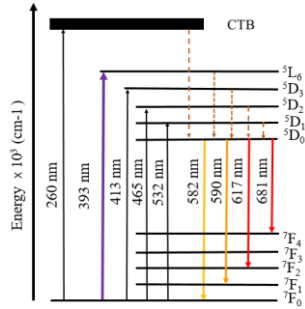


Figure 4. 8 Diagram illustrating energy levels and optical transitions in La3PO7:Eu3+ material

The R and β_{exp} values of the 5D0 – 7F2 transition increase when the sample annealing temperature increases from 500°C to 900°C. This result shows that the fluorescence efficiency of the red emission band and the asymmetry of the crystal field occupied by Eu3+ ions increase. In particular, for two specimens calcined at 800°C and 900°C, the β_{exp} values are both above 70%.

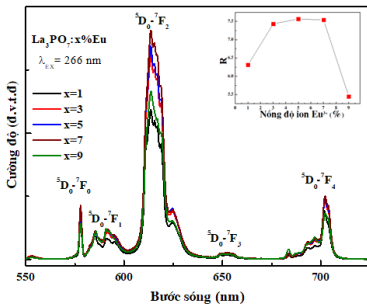


Figure 4. 11 Fluorescence spectra of La3PO7:x%Eu3+ samples

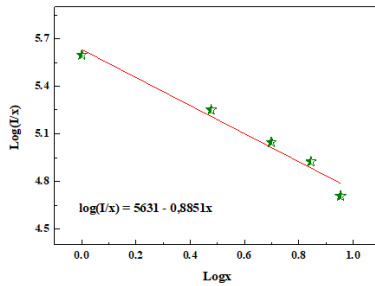


Figure 4. 10 Dependence of $\log(I/x)$ on $\log x$ of the material

Fluorescence quenching in concentration occurs when the Eu3+ doped ion concentration exceeds 5 mol%. Exchange interactions play a key role in this fluorescence quenching process

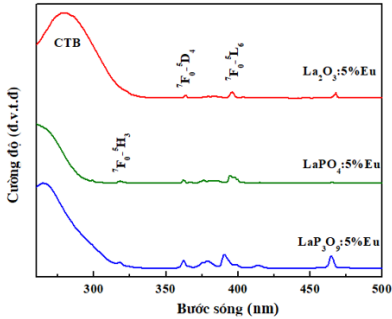


Figure 4. 12 Fluorescence excitation spectra of the materials $\text{La}_2\text{O}_3:5\%\text{Eu}^{3+}$, $\text{LaPO}_4:5\%\text{Eu}^{3+}$ and $\text{LaP}_3\text{O}_9:5\%\text{Eu}^{3+}$

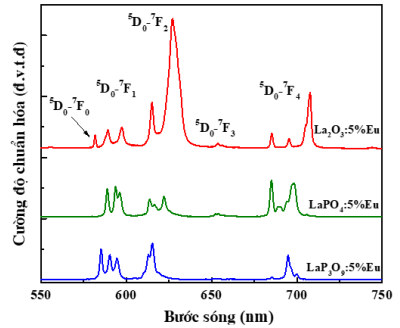


Figure 4. 13 Normalized fluorescence spectra of $\text{La}_2\text{O}_3:5\%\text{Eu}^{3+}$, $\text{LaPO}_4:5\%\text{Eu}^{3+}$ and $\text{LaP}_3\text{O}_9:5\%\text{Eu}^{3+}$

Table 4. 9 Experimental branching ratios of $5D_0-7F_{1,2,4}$ transitions of materials in Eu^{3+} doped $\text{La}_2\text{O}_3\text{-P}_2\text{O}_5$ matrix system

Samples	β_{exp} ($5D_0-7F_1$)(%)	β_{exp} ($5D_0-7F_2$)(%)	β_{exp} ($5D_0-7F_4$)(%)	R
$\text{La}_2\text{O}_3:5\%\text{Eu}^{3+}$	16,72	63,70	19,57	3,81
$\text{La}_3\text{PO}_7:5\%\text{Eu}^{3+}$	11,12	69,34	19,54	6,23
$\text{LaPO}_4:5\%\text{Eu}^{3+}$	42,93	31,54	25,53	0,73
$\text{LaP}_3\text{O}_9:5\%\text{Eu}^{3+}$	40,43	39,23	20,34	0,97
CAS: Eu^{3+} [99]				2,03
$\text{Gd}_3\text{PO}_7:5\%\text{Eu}^{3+}$	9,23	71,42	19,35	7,73
$\text{Sr}_3\text{B}_2\text{O}_6:\text{Eu}^{3+}$				2,67

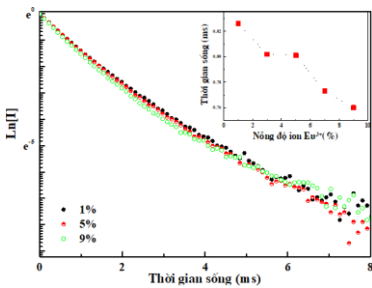


Figure 4. 15 Fluorescence attenuation curve of $\text{La}_3\text{PO}_7:x\%\text{Eu}^{3+}$ material

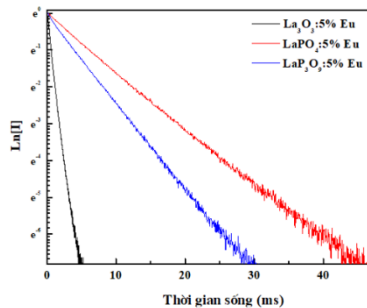


Figure 4. 14 Fluorescence attenuation curves of material samples $\text{La}_2\text{O}_3:5\%\text{Eu}^{3+}$, $\text{LaPO}_4:5\%\text{Eu}^{3+}$ and $\text{LaP}_3\text{O}_9:5\%\text{Eu}^{3+}$

With the material $\text{LaPO}_4:5\%\text{Eu}^{3+}$, the branching ratio of the 5D0-7F1 transition corresponding to the orange emission has the highest value of 42.93%, corresponding to $R = 0.73$. This result shows that Eu^{3+} ions occupy symmetric center positions in the LaPO_4 matrix. With the material $\text{LaP}_3\text{O}_9:5\%\text{Eu}^{3+}$, the branching ratio of transitions 5D0-7F1 and 5D0-7F2 has nearly the same value ($R=0.97$). With two materials $\text{La}_2\text{O}_3:5\%\text{Eu}^{3+}$ and $\text{La}_3\text{PO}_7:5\%\text{Eu}^{3+}$, the branching ratio of the 5D0-7F2 transition corresponding to red emission has a very high value. In particular, with $\text{La}_3\text{PO}_7:5\%\text{Eu}^{3+}$, this ratio has the highest value of 69.34%, corresponding to $R = 6.23$.

For $\text{La}_3\text{PO}_7:x\%\text{Eu}^{3+}$ samples, experiments show that when the Eu^{3+} ion concentration increases, the lifetime decreases. The fluorescence lifetime of $\text{La}_3\text{PO}_7:5\%\text{Eu}^{3+}$ material is 0.801 ms. The average fluorescence lifetime of $\text{La}_2\text{O}_3:5\%\text{Eu}^{3+}$ material samples is 0.584 ms shorter than the fluorescence lifetime of $\text{La}_3\text{PO}_7:5\%\text{Eu}^{3+}$ material. The calculated fluorescence lifetime result for the $\text{LaPO}_4:5\%\text{Eu}^{3+}$ sample is quite long with a value of 5.85 ms. The fluorescence lifetime of $\text{LaP}_3\text{O}_9:5\%\text{Eu}^{3+}$ material is 4.01 ms.

Table 4. 10 Values of Ω_2 , Ω_4 , fluorescence lifetime τ , quantum efficiency η and forced emission cross section $\sigma(\lambda_P)$ of 5D0 – 7F2 transition of $\text{La}_3\text{PO}_7:x\%\text{Eu}^{3+}$ material

Samples	Ω_2 ($\times 10^{-20}$ cm^2)	Ω_4 ($\times 10^{-20}$ cm^2)	$\sigma(\lambda_P)$ (10^{-22} cm^2)	τ_R (ms)	τ_{exp} (ms)	η (%)
$\text{La}_3\text{PO}_7:1\%\text{Eu}_{3+}$	8,84	3,66	28,1	1,300	0,826	63,54
$\text{La}_3\text{PO}_7:3\%\text{Eu}_{3+}$	9,21	3,81	26,7	1,246	0,802	64,37
$\text{La}_3\text{PO}_7:5\%\text{Eu}_{3+}$	9,22	3,82	29,3	1,244	0,801	64,39
$\text{La}_3\text{PO}_7:7\%\text{Eu}_{3+}$	9,37	3,81	27,6	1,228	0,773	62,95
$\text{La}_3\text{PO}_7:9\%\text{Eu}_{3+}$	8,76	3,69	29,7	1,440	0,760	52,78

Table 4. 11 Intensity parameters $\Omega\lambda$ of doped Eu^{3+} in $\text{La}_2\text{O}_3\text{-P}_2\text{O}_5$ matrix system

Samples	$\Omega_2 (\times 10^{-20} \text{ cm}^2)$	$\Omega_4 (\times 10^{-20} \text{ cm}^2)$
$\text{La}_2\text{O}_3:5\%\text{Eu}^{3+}$	6,07	3,83
$\text{La}_3\text{PO}_7:5\%\text{Eu}^{3+}$	9,22	3,82
$\text{LaPO}_4:5\%\text{Eu}^{3+}$	1,17	1,95
$\text{LaP}_3\text{O}_9:5\%\text{Eu}^{3+}$	1,50	1,71
$\text{Gd}_3\text{PO}_7:5\%\text{Eu}^{3+}$	11,12	6,71
$\text{Sr}_2\text{Al}_2\text{SiO}_7:\text{Eu}^{3+}$	3,60	1,68
$\text{Lu}_2\text{Ti}_2\text{O}_7:5\%\text{Eu}^{3+}$	5,02	2,58
$\text{YAlO}_3:\text{Eu}^{3+}$	2,11	6,53

The calculation results in Table 4.11 show that the Ω_2 value of $\text{La}_3\text{PO}_7:5\%\text{Eu}^{3+}$ material is 9.22, smaller than the Ω_2 value of $\text{Gd}_3\text{PO}_7:5\%\text{Eu}^{3+}$ (11.12) but larger than materials $\text{La}_2\text{O}_3:5\%\text{Eu}^{3+}$ and $\text{Lu}_2\text{Ti}_2\text{O}_7:5\%\text{Eu}^{3+}$, significantly larger than materials $\text{LaPO}_4:5\%\text{Eu}^{3+}$, $\text{LaP}_3\text{O}_9:5\%\text{Eu}^{3+}$, $\text{Sr}_2\text{Al}_2\text{SiO}_7:\text{Eu}^{3+}$ and $\text{YAlO}_3:\text{Eu}^{3+}$. In addition, the Ω_4 value of $\text{La}_3\text{PO}_7:\text{Eu}^{3+}$ material is equivalent to $\text{La}_2\text{O}_3:5\%\text{Eu}^{3+}$ material, much higher than $\text{LaPO}_4:5\%\text{Eu}^{3+}$, $\text{LaP}_3\text{O}_9:5\%\text{Eu}^{3+}$ materials. However, the hardness of $\text{La}_3\text{PO}_7:5\%\text{Eu}^{3+}$ material is higher than $\text{Gd}_3\text{PO}_7:5\%\text{Eu}^{3+}$ material.

Table 4. 12 Emission parameters of doped Eu^{3+} ions in the $\text{La}_2\text{O}_3\text{-P}_2\text{O}_5$ matrix system

Samples	$\beta_{\text{exp}} (\%)$ $^5\text{D}_0 \rightarrow ^7\text{F}_2$	$\beta_{\text{cal}} (\%)$ $^5\text{D}_0 \rightarrow ^7\text{F}_2$	$\tau_{\text{R}} (\text{ms})$	$\tau_{\text{exp}} (\text{ms})$	$\eta (\%)$
$\text{La}_2\text{O}_3:5\%\text{Eu}^{3+}$	63,70	63,83	1,800	0,584	32,44
$\text{La}_3\text{PO}_7:5\%\text{Eu}^{3+}$	69,34	70,14	1,244	0,801	64,39
$\text{LaPO}_4:5\%\text{Eu}^{3+}$	31,54	31,33	8,271	5,850	70,73
$\text{LaP}_3\text{O}_9:5\%\text{Eu}^{3+}$	39,23	39,02	7,789	4,013	51,52

Emission parameters of the materials in the La₂O₃-P₂O₅ matrix system: La₃PO₇:5%Eu³⁺ material has a very high branching ratio of the 5D₀→7F₂ transition (69.34%), a larger value for The remaining materials are in the same matrix system and there is not much difference between the experimental and theoretical values. Besides, in terms of quantum efficiency, this value is the highest corresponding to the material LaPO₄:5%Eu³⁺ (70.73%), followed by the material La₃PO₇:5%Eu³⁺ (64.39%).

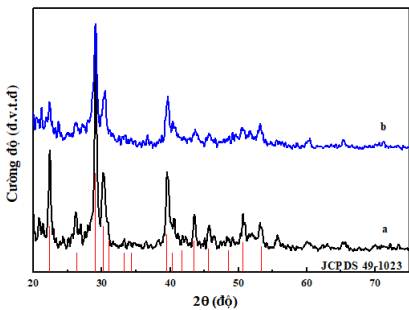


Figure 4. 17 X-ray diffraction pattern of materials La₃PO₇:5%Eu (a) and La₃PO₇:5%Eu,4%Bi (b)

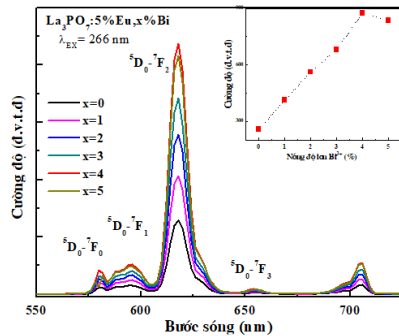


Figure 4. 16 Fluorescence spectrum of La₃PO₇:5%Eu,x%Bi material

XRD results show that La₃PO₇:5%Eu,4%Bi material was successfully synthesized by explosive reaction method. The average crystal size calculated according to the Debye-Scherrer formula is about 30 nm. Fluorescence spectrum Figure 4.23 shows that the fluorescence intensity gradually increases when the Bi³⁺ ion concentration increases from 1 to 4 mol% but shows signs of decline when the Bi³⁺ ion concentration is 5 mol%. The main interaction mechanism between Eu³⁺ and Bi³⁺ ions is exchange interaction.

Table 4. 2 Intensity parameters $\Omega_{2,4}$ of Eu^{3+} and branching ratio of ${}^5\text{D}_0\text{-}{}^7\text{F}_2$ transition of $\text{La}_3\text{PO}_7:5\%\text{Eu},x\%\text{Bi}$ materials

Samples $\text{La}_3\text{PO}_7:5\%\text{Eu},x\%\text{Bi}$	$\Omega_2 (\times 10^{-20} \text{ cm}^2)$	$\Omega_4 (\times 10^{-20} \text{ cm}^2)$	$\beta_{\text{exp}}(\%)$ ${}^5\text{D}_0\text{-}{}^7\text{F}_2$
x=0	9,15	3,88	69,34
x=1	9,54	3,85	70,08
x=2	9,97	3,97	70,14
x=3	10,06	3,99	70,40
x=4	10,05	3,98	70,32
x=5	8,92	3,67	69,83

CONCLUSION

Basically, the project "Synthesis and studying optical properties of Ln_3PO_7 ($\text{Ln}=\text{La}, \text{Gd}$) nanomaterials doped with Eu^{3+} ions" has completed the initial research goal with results and contributions as:

1. Successfully manufactured two types of materials $\text{La}_3\text{PO}_7:\text{Eu}^{3+}$ and $\text{Gd}_3\text{PO}_7:\text{Eu}^{3+}$ by explosive reaction method, using urea as fuel for the reaction. Develop a sample manufacturing process. The results of structural and morphological studies show that the material has a monoclinic structure, the material particles are quasi-spherical in shape with an average size in the range of 20-30 nm, responding well to spectroscopic studies. .
2. The results of fluorescence spectrum analysis and fluorescence lifetime measurements of the two materials $\text{La}_3\text{PO}_7:\text{Eu}^{3+}$ and $\text{Gd}_3\text{PO}_7:\text{Eu}^{3+}$ have shown that Eu^{3+} ion occupies at least two different positions in the

background lattice, a quenching phenomenon. Fluorescence occurs when the Eu^{3+} ion concentration exceeds 5 mol%, the fluorescence quenching mechanism is determined to be exchange interaction. Determine the experimental lifetime of the samples. Observe the electron - phonon interaction effect in $\text{La}_3\text{PO}_7:5\%\text{Eu}^{3+}$ material through sideband phonon spectrum, calculate the electron - phonon coupling constant.

3. For the first time, the optical properties of four materials in the $\text{Ln}_2\text{O}_3\text{-P}_2\text{O}_5$ lattice system ($\text{Ln} = \text{La}, \text{Gd}$) are compared through the Judd-Ofelt theory. Determining the intensity parameters $\Omega_{2,4}$, the asymmetry of the ligand field and the covalence of the RE^{3+} -ligand bond in the two materials $\text{La}_3\text{PO}_7:\text{Eu}^{3+}$ and $\text{Gd}_3\text{PO}_7:\text{Eu}^{3+}$ are higher than other materials in the base network system. $\text{Ln}_2\text{O}_3\text{-P}_2\text{O}_5$ ($\text{Ln} = \text{La}, \text{Gd}$). However, the "hardness" of the environment around the Eu^{3+} ion is lower. Besides, the emission parameters: forced emission cross section, branching ratio, quantum efficiency are also determined. The results show that the quantum efficiency and branching ratio of the ${}^5\text{D}_0 - {}^7\text{F}_2$ transition of the two materials $\text{La}_3\text{PO}_7:5\%\text{Eu}^{3+}$ and $\text{Gd}_3\text{PO}_7:5\%\text{Eu}^{3+}$ have high values, suitable for exploiting applications. red light irradiation.

4. Researched the influence of Bi^{3+} ions on the optical properties of two materials $\text{La}_3\text{PO}_7:\text{Eu}^{3+}$ and $\text{Gd}_3\text{PO}_7:\text{Eu}^{3+}$. The results show that there is resonance energy transfer from Bi^{3+} to Eu^{3+} which helps significantly improve the fluorescence intensity.

NEW CONTRIBUTIONS OF THE THESIS

- 1- Synthesized luminescent nanomaterials $\text{La}_3\text{PO}_7:\text{Eu}^{3+}$, $\text{Gd}_3\text{PO}_7:\text{Eu}^{3+}$ by explosive reaction method, using urea as fuel.
- 2- Research the influence of factors: synthesis temperature, doping ion concentration on the optical properties of two materials $\text{La}_3\text{PO}_7:\text{Eu}^{3+}$, $\text{Gd}_3\text{PO}_7:\text{Eu}^{3+}$.
- 3- Research the influence of Bi^{3+} ions on the optical properties of two materials $\text{La}_3\text{PO}_7:\text{Eu}^{3+}$, $\text{Gd}_3\text{PO}_7:\text{Eu}^{3+}$.
- 4- Compare the optical properties between materials in the Eu^{3+} -doped $\text{Ln}_2\text{O}_3\text{-P}_2\text{O}_5$ ($\text{Ln}=\text{La}, \text{Gd}$) lattice system with specific data by applying the Judd-Ofelt theory.

PUBLICATION LIST

1. Ngo K. K. Minh, Tran B. Luan, Lam T. K. Giang, Nguyen T. Thanh, Tran T. K. Chi, Dariusz Hreniak, Ngo Q. Luan, Nguyen Vu, 2020, Preparation and Optical Properties of $\text{La}_3\text{PO}_7:\text{Eu}^{3+}$ Nanophosphors Synthesized by Combustion Method, *Materials Transactions*, 61(8), pp. 1564-1568.
2. Khac Khong Minh Ngo, Vu Nguyen, Thi Kieu Giang Lam, Thi Khuyen Hoang, Manh Tien Dinh, Mariusz Stefanski, Karina Grzeszkiewicz, Dariusz Hreniak, 2020, Effect of calcination temperature on optical properties of $\text{Gd}_3\text{PO}_7:\text{Eu}^{3+}$ nanophosphors synthesised by the combustion method, *Int. J. Nanotechnol*, 17(7-10), 623-635
3. Ngo Khac Khong Minh, Lam Thi Kieu Giang, Nguyen Trong Nghia, Nguyen Vu, 2018, Properties emission of $\text{La}_3\text{PO}_7:\text{Eu}^{3+}$, Bi^{3+} nanophosphors synthesized by combustion method, *Vietnam J. Chem*, 56 (6E2), 300-303.
4. Ngô Khắc Không Minh, Ngô Quốc Luân, Phan Thanh Phường, Phạm Thanh Tùng, Lâm Thị Kiều Giang, Nguyễn Vũ, 2023, Nghiên cứu tính chất quang của vật liệu nano $\text{Gd}_2\text{O}_3:\text{Eu}$ bằng thuyết Judd-Ofelt, *Tạp chí xúc tác và hấp phụ Việt Nam*, 12(1), 106-110.